Inorg. Chem. **2003**, *42*, 482–491

Supramolecular Assembly and Solution Properties of Bis(bipyridyl)ruthenium(II) Coordination Complexes of Aryl(2-pyridyl)methanones

Daniel L. Reger,* James R. Gardinier, Mark D. Smith, and Perry J. Pellechia

Department of Chemistry and Biochemistry, University of South Carolina, Columbia, South Carolina 29208

Received September 10, 2002

A series of mono- and bis(2-pyridyl)-arylmethanone ligands were prepared by utilizing the reaction between either bromobenzonitrile or dicyanobenzene and 2-lithiopyridine in either a 1:1 or a 2:1 mol ratio, respectively. They react with $[Ru(bpy)_2(EtOH)_2][PF_6]_2$ to yield the new complexes $[N,O\text{-}PhC(O)(2\text{-}py)Ru(bpy)_2][PF_6]_2$ (**6**), $[p\text{-}N,O\text{-}BrC_6H_4C(O)(2\text{-}py)Ru(bpy)_2][PF_6]_2$ (**7**), $[m\text{-}N,O\text{-}BrC_6H_4C(O)(2\text{-}py)Ru(bpy)_2][PF_6]_2$ (**8**), $\{p\text{-}[N,O\text{-}C(O)(2\text{-}py)_2Ru(bpy)_2]_2(C_6H_4)\}[PF_6]_4$ (**9**), and $\{m\text{-}[N,O\text{-}C(O)(2\text{-}py)_2Ru(bpy)_2]_2(C_6H_4)\}[PF_6]_4$ (**10**). The solid state structures of **6** and **7** show that the octahedral cations are arranged in sinusoidal chains by π–π stacking and CH–π interactions between bipyridyl groups. Substitution of bromine for hydrogen at the para position of the aryl group in **7** causes the aryl group to become involved in π–π stacking interactions that organize the chains into a sheet structure. The complicated ^1H and ^{13}C NMR spectra of the complexes have been fully assigned using 2D methods. The optical spectra show two absorption maxima near 434 and 564 nm due to MLCT transitions. The compounds were found to be nonluminescent. Electrochemical data acquired for CH_3CN solutions of the bimetallic derivatives indicate that there is no electronic communication between metal centers mediated either through space or through ligand orbitals. Crystallographic information: **6**·0.5CH_3CN is monoclinic, $C2/c$, $a = 24.3474(11)$ Å, $b = 13.7721(6)$ Å, $c = 21.3184(10)$ Å, $\beta = 103.9920(10)°$, $Z = 8$; **7** is monoclinic, $P2_1/c$, $a = 10.6639(11)$ Å, $b = 23.690(3)$ Å, $c = 13.7634(14)$ Å, $\beta = 91.440(2)°$, $Z = 4$.

Introduction

Interest in the study of ruthenium polypyridyl complexes has been driven by the ability for such compounds to be employed in the fabrication of light-emitting electrochemical cells[1] and by the promise of their use in future technologies such as photoswitchable memory devices,[2] in the area of artificial photosynthesis,[3] in light-harvesting dendrimers,[4] or in the area of chemotherapeutics.[5] The favorable photophysical and electrochemical properties of these compounds arise as a result of the electronic transitions between the metal center and various ligands with low energy π^* orbitals.[6] It is becoming evident that interactions between either the pyridyl-based or other ruthenium-bound aromatic ligands and their surrounding environment will play a crucial role in the development of more sophisticated and presumably better performing technologies.[7] As a result, the study of the supramolecular chemistry of these species will allow a more accurate understanding of the relationship between structure and function in ruthenium polypyridyl compounds.[4,8] During the course of our ongoing research efforts in developing supramolecular materials based on bitopic ligands,[9] we have prepared mono- and bis(2-pyridyl)-arylmethanones such as

* To whom correspondence should be addressed. E-mail: reger@mail.chem.sc.edu.

(1) Buda, M.; Kalyuzhny, G.; Bard, A. J. *J. Am. Chem. Soc.* **2002**, *124*, 6090.
(2) Tyson, D. S.; Bignozzi, C. A.; Castellano, F. N. *J. Am. Chem. Soc.* **2002**, *124*, 4562.
(3) Abrahamsson, M. L. A.; Baudin, H. B.; Tran, A.; Philouze, C.; Berg, K. E.; Raymond-Johansson, M. K.; Akermark, B.; Sun, L.; Styring, S.; Hammarstrom, L. *Inorg. Chem.* **2002**, *41*, 1534.
(4) Balzani, V.; Campagna, S.; Denti, G.; Juris, A.; Serroni, S.; Venturi, M. *Acc. Chem. Res.* **1998**, *31*, 26.
(5) See for instance: Erkkila, K. E.; Odom, D. T.; Barton, J. K. *Chem. Rev.* **1999**, *99*, 2777.
(6) Juris, A.; Balzani, F.; Barigelletti V.; Campagna, S.; Belser, P.; von Zelewsky, A. *Coord. Chem. Rev.* **1988**, *84*, 85.
(7) Balzani, V.; Juris, A.; Venturi, M.; Campagna, C.; Serroni, S. *Chem. Rev.* **1996**, *96*, 759.
(8) (a) Wu, F.; Riesgo, E.; Pavalova, A.; Kipp, R. A.; Schmehl, R. H.; Thummel, R. P. *Inorg. Chem.* **1999**, *38*, 5620. (b) Breu, J.; Domel, H.; Stoll, A. *Eur. J. Inorg. Chem.* **2000**, 2401. (c) Gut, D.; Rudi, A.; Kopilov, J.; Goldberg, I.; Kol, M. *J. Am. Chem. Soc.* **2002**, *124*, 5449.

10.1021/ic026018n CCC: $25.00
Published on Web 12/20/2002

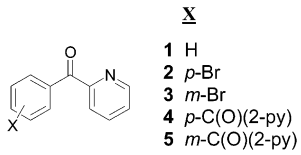

Figure 1. Aryl(2-pyridyl)methanones.

those depicted in Figure 1.[10] These arylpyridylmethanones represent a potentially interesting class of ligands for ruthenium because the "hemilabile" nature of neutral bidentate N,O ligands[11] may give rise to optical-switching properties as a result of ligand dissociation and might allow the future introduction of catalytic capabilities into supramolecular systems. In this report, we present our initial findings concerning the nature of bis(2,2′-bipyridyl)ruthenium(II) complexes of aryl(pyridyl)methanones.

Experimental Section

Materials. Solvents for synthetic procedures and spectroscopic and electrochemical studies were dried by conventional methods and distilled under N_2 atmosphere immediately prior to use. All manipulations involving air- and moisture-sensitive compounds were carried out either in the drybox under a purified N_2 atmosphere or by using standard Schlenk techniques. $Ru(bpy)_2Cl_2 \cdot 2H_2O$ was purchased from Strem Chemicals. The compound 2-benzoylpyridine, PhC(O)(2-py) (**1**), and all other reagents were used as received from Aldrich Chemical Co. Silica gel (0.040−0.063 mm, 230−400 mesh) used for chromatographic separations was purchased from Fischer Scientific.

Physical Measurements. Robertson Microlit Laboratories performed all elemental analyses. Melting point determinations were made on samples contained in sealed glass capillaries by using an Electrothermal 9100 apparatus and are uncorrected. Infrared spectra of approximately 0.5 mM CH_2Cl_2 solutions of the desired compounds contained between NaBr plates were acquired with a Nicolet 5DXB FTIR spectrometer. Mass spectrometric measurements recorded in ESI(+) mode were obtained on a Micromass Q-Tof spectrometer whereas those performed by using direct probe analyses were made on a VG 70S instrument. Absorption measurements were recorded with a JASCO V-530 spectrophotometer. Emission spectra were recorded by using a JASCO FP-6500 spectrofluorometer. Electrochemical measurements were collected with a BAS CV-50W instrument at a scan rate of 200 mV/s for samples as 0.1 mM CH_3CN solutions with 0.1 M NBu_4PF_6 as the supporting electrolyte, and a three-electrode cell composed of a Ag/AgCl reference electrode, a platinum working electrode, and a glassy carbon counter electrode. The reported values were corrected to the ferrocene couple (+0.42 V vs SCE) as an external standard. NMR spectra were recorded by using either a Varian Mercury 400 or a Varian Inova 500 instrument, as noted within the text. Chemical shifts were referenced to solvent resonances at either δ_H 7.27, δ_C 77.23 for $CDCl_3$ or δ_H 1.93, δ_C 1.39 for CD_3CN.

Preparation of the Aryl(2-pyridyl)methanones, 2−5. The preparation of each of the aryl(2-pyridyl)methanones **2**−**5** was achieved by following a procedure analogous to that described in the next paragraph in detail for **2**. The isolated yield of spectroscopically (^{1}H NMR) pure product obtained from the stated quantity of reagents, and the solvent system(s) used for chromatographic separation (silica gel) of the crude product mixture, is given for compounds **3**−**5**.

***p*-BrC$_6$H$_4$[C(O)(2-py)], (2).** A 250 mL three-necked flask fitted with a magnetic stir bar was connected to a sidearm dumper that contained 4.2 g (23 mmol) of *p*-$BrC_6H_4(CN)$, to a pressure equalizing addition funnel, and to the Schlenk line by a vacuum adapter. The apparatus was purged with N_2 for 30 min, and then 2.2 mL (23 mmol, 1.657 g/mL) of 2-bromopyridine and 100 mL of Et_2O were added sequentially by syringe to the flask via the addition funnel. Next, 14 mL of a 1.6 M solution (23 mmol) of Li^{n}Bu in hexanes and 20 mL of Et_2O were transferred to the addition funnel. The flask was cooled to −78 °C, and the Li^{n}Bu solution was added dropwise to the ethereal 2-bromopyridine solution. After complete addition, the resulting red solution (of 2-lithiopyridine) was stirred 20 min, and then *p*-$BrC_6H_4(CN)$ was added in several portions over 5 min. The reaction mixture was stirred at −78 °C for 1 h, the cold bath was removed, and the mixture was allowed to warm to room temperature with stirring over the course of 4 h. The resulting red-violet slurry was poured into 100 mL of cold (0 °C) 3 M HCl. After the mixture had been stirred 20 min, the organic and aqueous fractions were separated, 3 M NaOH was added to the aqueous fraction until the mixture was slightly basic to litmus, and the aqueous fraction was extracted with three 100 mL portions of CH_2Cl_2. The combined organic fractions were dried over $MgSO_4$ and filtered, and solvent was removed by rotary evaporation to leave a dark orange oil. The oil was loaded onto a silica gel column and was eluted first with CH_2Cl_2/hexanes 1:1 until a sample of the eluent spotted on a TLC plate turned yellow-brown on exposure to UV lamp (after 400 mL collected). The column was then eluted with 4:1 CH_2Cl_2/hexanes to give the desired fraction in a pale yellow band prior to a yellow-orange band.[12a] Evaporation of the solvent from the pale yellow band followed by trituration of the resulting pale yellow oil with 10 mL of Et_2O afforded 3.9 g (65%) of **2** as a pale yellow solid; mp 45−47 °C (lit. 48−50,[12b] 37−40 °C[12c]). IR (cm^{-1}) ν_{co} 1667 (br, vs). UV−vis (nm, CH_3CN) λ_{max} (log ϵ) 226 (4.89), 274 (4.33). ^{1}H NMR (400 MHz, $CDCl_3$) 8.72 (d, 1 H, J = 5 Hz, H_6-py), 8.08 (ddd, 1 H, H_3-py), 7.99, 7.64 (m, m; 2, 2 H; Ph, AA′BB′), 7.92 (ddd, J = 7.8, 7.8, 1 Hz, 1 H, H_4-py), 7.50 (ddd, J = 7.8, 5, 1 Hz, 1 H, H_5-py). ^{13}C NMR (101.62 MHz, $CDCl_3$) 192.8 (C═O), 154.8 (C_2-py), 148.7 (C_6-py), 137.4 (C_4-py), 135.2 (C_1-Ph), 132.8 (C_3-Ph), 131.6 (C_2-Ph), 128.4 (C_4-Ph), 126.7 (C_3-py), 124.9 (C_5-py). HRMS direct probe (*m*/*z*): $[M - H]^+$ calcd for $C_{12}H_7BrNO$, 260.9789; found, 260.9781. Direct probe MS *m*/*z* (rel int %) [assgn]: 262, 261 (64) [M, M − H, overlapping]$^+$, 233 (100) $[M - CO]^+$, 183 (81) $[M - Br]^+$, 154 (66) $[C_6H_3Br]^+$, 104 (10) $[C(O)C_6H_4]^+$, 76 (44) $[C_6H_4]^+$.

(9) (a) Reger, D. L.; Brown, K. J.; Smith, M. D. *J. Organomet. Chem.* **2002**, *658*, 50. (b) Reger, D. L.; Grattan, T. C.; Brown, K. J.; Little, C. A.; Lamba, J. J. S.; Rheingold, A. L.; Sommer, R. D. *J. Organomet. Chem.* **2000**, *607*, 120. (c) Reger, D. L.; Wright, T. D.; Semeniuc, R. F.; Grattan, T. C.; Smith, M. D. *Inorg. Chem.* **2001**, *40*, 6212. (d) Reger, D. L.; Semeniuc, R. F.; Smith, M. D. *Eur. J. Inorg. Chem.* **2002**, 543.

(10) The, K. I.; Peterson, L. K.; Kielmann, E. *Can. J. Chem.* **1973**, *51*, 2448.

(11) Bellachioma, G.; Cardaci, G.; Gramlich, V.; Macchioni, A.; Valentini, M.; Zuccaccia, C. *Organometallics* **1998**, *17*, 5025.

(12) (a) Further elution of the column with Et_2O affords a yellow-orange band that contained 0.16 g (0.44 mmol) of 4-bromo-4′-(2-pyridinecarbonyl)benzophenone. Pale yellow solid. Mp 167−170 °C w/dec. IR ν_{co} 1664 (br, vs). ^{1}H NMR (400 MHz, $CDCl_3$) 8.76 (s, 1 H, J = 4.5 Hz, H_6-py), 8.19 (d, J_{AB} = 8.1 Hz, 2 H, H_3-Ph), 8.15 (d, J = 7.8 Hz, 1 H, H_3-py), 7.96 (ddd, J = 7.8, 7.8, 1 Hz, 1 H, H_4-py), 7.87 (d, J_{AB} = 8.1 Hz, 2 H, H_2-Ph), 7.73 (d, $J_{A'B'}$ = 8.7 Hz, 2 H, $H_{3'}$-Ph), 7.66 (d, $J_{A'B'}$ = 8.7 Hz, 2 H, $H_{2'}$-Ph). ^{13}C NMR (101.62 MHz, $CDCl_3$) 195.3, 193.3, 154.5, 148.9, 140.6, 139.7, 137.5, 136.0, 132.0, 131.8, 131.1, 129.6, 128.3, 126.9, 125.0. (b) Bruce, R. B.; Turnbull, L. B.; Newman, J. H.; Pitts, J. E. *J. Med. Chem.* **1968**, *11*, 1031. (c) Glover, E. E.; Adamson, J. *J. Chem. Soc. C* **1971**, 861.

***m*-BrC$_6$H$_4$[C(O)(2-py)] (3).** A 3.5 g (72% yield) sample of **3** as a colorless solid was obtained from the reaction between 3.4 g (19 mmol) of *m*-Br(C$_6$H$_4$)CN, 1.9 mL (20 mmol) of (2-Br)py, and 12 mL of Li^{n}Bu (19 mmol, 1.6 M hexanes) in 120 mL of Et$_2$O and after evaporation of the second band eluted from a silica gel column using 3:1 CH$_2$Cl$_2$/hexanes as the eluent; $R_f = 0.6$ silica plate. Mp 82−84 °C. Anal. Calcd (Obsd) for C$_{12}$H$_8$BrNO: C, 54.99 (54.86); H, 3.08 (2.92); N, 5.34 (5.05). IR(cm^{-1}) ν_{co} 1667 (br, vs). UV−vis (nm, CH$_3$CN) λ_{max} (log ϵ) 236 (4.96), 280 (3.77). ^{1}H NMR (400 MHz, CDCl$_3$) 8.74 (d, 1 H, $J = 5$ Hz, H$_6$-py), 8.23 (m, 1 H, Ph), 8.08 (ddd, 1 H, H$_3$-py), 8.23 (m, 1 H, Ph), 7.93 (ddd, $J = 7.8$, 7.8, 1 Hz, 1 H, H$_4$-py), 7.72 (m, 1 H, Ph), 7.53 (ddd, $J = 7.8$, 5, 1 Hz, 1 H, H$_5$-py), 7.38 (m, 1 H, Ph). ^{13}C NMR (101.62 MHz, CDCl$_3$) 192.5 (C═O), 154.5 (C$_2$-py), 148.8 (C$_6$-py), 138.3 (C$_3$-Ph), 137.4 (C$_4$-py), 135.9 (C$_6$-Ph), 134.0 (C$_2$-Ph), 129.9 (C$_5$-Ph), 129.8 (C$_4$-Ph), 126.8 (C$_3$-py), 124.9 (C$_5$-py), 122.5 (C$_1$-Ph). HRMS direct probe (*m*/*z*): [M − H]$^+$ calcd for C$_{12}$H$_7$BrNO, 260.9789; found, 260.9786. Direct probe MS *m*/*z* (rel int %) [assgn]: 262, 261 (62) [M, M − H, overlapping]$^+$, 233 (81) [M − CO]$^+$, 183 (81) [M − Br]$^+$, 154 (100) [C$_6$H$_3$Br]$^+$, 76 (82)[C$_6$H$_4$]$^+$.

***p*-C$_6$H$_4$[C(O)(2-py)]$_2$ (4).** A 1.9 g (33% yield) sample of **4** was isolated from the product mixture obtained from the reaction between 2.5 g (20 mmol) of 1,4-(CN)$_2$C$_6$H$_4$, 4.0 mL (40 mmol) of (2-Br)py, and 25 mL of Li^{n}Bu (40 mmol, 1.6 M hexanes) in 150 mL of toluene (the mixture was stirred for 16 h). Purification was achieved by column chromatography (SiO$_2$) where two bands of unidentified impurities were first removed by using 3:1 CHCl$_3$/Et$_2$O as the eluent. The third band contained the desired product ($R_f = 0.55$, spot on silica plate turns violet immediately upon exposure to 254 nm light) and an orange-yellow impurity. After the solvent was removed by rotary evaporation and the orange-yellow impurity was separated by washing the crude mixture with Et$_2$O, **4** was left as a pale yellow solid; mp 172−174 °C. IR(cm^{-1}) ν_{co} 1669 (br, vs). UV−vis (nm, CH$_3$CN) λ_{max} (log ϵ) 232 (5.19), 282 (4.36). ^{1}H NMR (400 MHz, CDCl$_3$) 8.73 (d, 1 H, $J = 5$ Hz, H$_6$-py), 8.17 (2, 4 H, Ph), 8.10 (dd, 7.8, 1 Hz, 1 H, H$_3$-py), 7.92 (ddd, $J = 7.8$, 7.8, 1 Hz, 1 H, H$_4$-py), 7.51 (ddd, $J = 7.8$, 5, 1 Hz, 1 H, H$_5$-py). ^{13}C NMR (101.62 MHz, CDCl$_3$) 193.5 (C═O), 154.7 (C$_2$-py), 148.9 (C$_6$-py), 139.8 (C$_i$-Ph), 137.4 (C$_4$-py), 130.8 (C$_o$-Ph), 126.8 (C$_3$-py), 124.9 (C$_5$-py). HRMS direct probe (*m*/*z*): M$^+$ calcd for C$_{18}$H$_{12}$N$_2$O$_2$, 288.0899; found, 288.0892. Direct probe MS *m*/*z* (rel int %) [assgn]: 288 (80) [M]$^+$, 260 (50) [M − CO]$^+$, 232 (14) [M − 2CO]$^+$, 210 (77) [M − py]$^+$, 182 (100) [M − C(O)py]$^+$, 154 (28) [Ph(py)]$^+$, 78 (20) [py]$^+$.

***m*-C$_6$H$_4$[C(O)(2-py)]$_2$ (5).** A 1.5 g (16% based on dicyanobenzene) portion of pure **5** as colorless needles was obtained from the reaction between 4.0 g (32 mmol) of 1,3-dicyanobenzene, 6.0 mL (63 mmol) of 2-bromopyridine, and 40 mL of Li^{n}Bu (64 mmol, 1.6 M hexane solution) in 120 mL of 50% toluene/THF. Column chromatography (SiO$_2$, Et$_2$O) was used to separate the desired compound as the minor component of the initial product mixture. The major component of the initial product mixture (dark red orange oil) could not be conclusively identified. The initial bright orange band that contained the unidentified dark red orange oil was discarded. The following yellow band ($R_f = 0.7$ on TLC plate) contained the desired product (that slowly precipitates from the solution). Numerous attempts to improve the isolated yields by varying conditions such as the reaction medium, time, or temperature were not successful. Mp 134−135 °C (lit.[15] 114−115 °C). IR(cm^{-1}) ν_{co} 1670 (br, vs). UV−vis (CH$_3$CN) λ_{max} (log ϵ) 234 (5.18), 282 (3.70). ^{1}H NMR (400 MHz, CDCl$_3$) 8.82 (s, 1H, H$_2$-Ph), 8.74 (d, 1 H, $J = 5$ Hz, H$_6$-py), 8.35 (d, 2 H, $J = 8.8$ Hz, H$_{4,6}$-Ph), 8.10 (dd, 7.8, 1 Hz, H, H$_3$-py), 7.93 (ddd, $J = 7.8$, 7.8, 1 Hz, 1 H, H$_4$-py), 7.64 (t, 1 H, $J = 8.8$ Hz, C$_5$-Ph), 7.51 (ddd, $J = 7.8$, 5, 1 Hz, 1 H, H$_5$-py). ^{13}C NMR (101.62 MHz, CDCl$_3$) 193.1 (C═O), 154.8 (C$_2$-py), 148.9 (C$_6$-py), 137.3 (C$_4$-py), 136.4 (C$_i$-Ph), 135.2 (C$_{o,p}$-Ph), 134.1 (C$_{o,o}$-Ph), 128.3 (C$_{m,m}$-Ph), 126.6 (C$_3$-py), 124.9 (C$_5$-py). Direct probe MS *m*/*z* (rel int %) [assgn]: 288 (18) [M]$^+$, 232 (3) [M − 2CO]$^+$, 210 (16) [M − py]$^+$, 182 (100) [M − C(O)py]$^+$, 154 (11) [M − 2COpy]$^+$, 78 (20) [py]$^+$.

Synthesis of Metal Complexes. Each of the ruthenium derivatives **6**−**10** was prepared by heating "[Ru(bpy)$_2$(EtOH)$_2$][PF$_6$]$_2$" (formed in situ on a 0.5 mmol scale by heating a mixture of 1.0 mmol of AgPF$_6$ and 0.5 mmol of Ru(bpy)$_2$Cl$_2$·2H$_2$O in 50 mL of EtOH at reflux for 2 h) and either an excess of the monotopic aryl-(2-pyridyl)methanone (**1**−**3**) or a limiting amount (<0.25 mmol) of bitopic bis[(2-pyridyl)methanone]benzene (**4** or **5**) under nitrogen for 16 h. The analytically pure compounds as polycrystalline solids were isolated after cooling the violet-black product mixture to 0 °C, filtering, washing the insoluble portion with ice-cold ethanol and then with Et$_2$O followed by benzene, and drying in a 150 °C oven for 30 min. By concentrating the mother liquor and washings from the filtration step, additional batches of product can be recovered such that the total isolated yield of the desired compound is typically between 60% and 75%. Isolated yields and characterization data for compounds **6**−**10** can be found in Tables 2, 3, 5, and 6. The compound [Ru(bpy)$_3$][PF$_6$]$_2$ was obtained in a 71% yield by following the described methodology. The species [Ru(bpy)$_2$(CD$_3$CN)$_2$][PF$_6$]$_2$ used for NMR spectroscopic studies (vide infra) was prepared by heating a mixture of 11 mg (21 μmol) of Ru(bpy)$_2$Cl$_2$·2H$_2$O, 11 mg (42 μmol) of AgPF$_6$, and 2 mL of CD$_3$CN to reflux 2 h, and then transferring the solution into an NMR tube by filtration under nitrogen.

X-ray Crystallography. Satisfactory single crystals of **6**·0.5CH$_3$CN and **7** were grown by vapor diffusion of Et$_2$O into CH$_3$CN solutions of each compound. An irregular brown block of **6**·0.5CH$_3$CN and a brown rhombic plate of **7** were each mounted on the end of a thin glass fiber using inert oil. For each compound, X-ray intensity data covering the entire sphere of reciprocal space were measured at 150(1) K on a Bruker SMART APEX CCD-based diffractometer (Mo Kα radiation, $\lambda = 0.71073$ Å). The raw data frames were integrated with SAINT+,[13] which also applied corrections for Lorentz and polarization effects. The final unit cell parameters were based on the least-squares refinement of 8296 reflections obtained for **6**·0.5CH$_3$CN and of 7532 reflections obtained for **7** each with $I > 5\sigma(I)$ from the respective data sets. Analysis of each data set showed negligible crystal decay during collection. An empirical absorption correction based on the multiple measurements of equivalent reflections was applied for each with the program SADABS.[14] For **6**·0.5CH$_3$CN, systematic absences in the intensity data were consistent with the space groups *Cc* and *C*2/*c*; intensity statistics indicated centricity. The structure was solved in *C*2/*c* by a combination of direct methods and difference Fourier syntheses and refined by full-matrix least-squares against F^2, using the SHELXTL software package.[14] All atoms of the cation and anions are on positions of general crystallographic symmetry. An acetonitrile molecule of crystallization lies on a 2-fold axis of rotation. For **7**, systematic absences in the intensity data were consistent with the space group $P2_1/c$. The structure was solved and refined by the methods described here. No species present

(13) *SMART Version 5.625, SAINT+ Version 6.02a, and SADABS*; Bruker Analytical X-ray Systems, Inc.: Madison, WI, 1998.

(14) Sheldrick, G. M. *SHELXTL, Version 5.1*; Bruker Analytical X-ray Systems, Inc.: Madison, WI, 1997.

(15) Canty, A. J.; Minchin, N. J.; Skelton, B. W.; White, A. H. *J. Chem. Soc., Dalton Trans.* **1987**, 1477.

Table 1. Summary of Crystal Data, Data Collected, and Structure Refinement Parameters for [*N*,*O*-PhC(O)(2-py)Ru(bpy)$_2$][PF$_6$]$_2$·0.5CH$_3$CN, **6**·0.5CH$_3$CN, and [*p*-*N*,*O*-BrC$_6$H$_4$C(O)(2-py)Ru(bpy)$_2$][PF$_6$]$_2$, **7**

	6·0.5CH$_3$CN	**7**
formula	$C_{33}H_{26.5}F_{12}N_{5.5}OP_2Ru$	$C_{32}H_{24}BrF_{12}N_5OP_2Ru$
fw	907.11	965.48
cryst syst	monoclinic	monoclinic
space group	*C*2/*c*	*P*2$_1$/*c*
a, Å	24.3474(11)	10.6639(11)
b, Å	13.7721(6)	23.690(3)
c, Å	21.3184(10)	13.7634(14)
β, (deg)	103.9920(10)	91.440(2)
V, Å^3	6936.3(5)	3475.9(6)
Z	8	4
cryst dimens, mm^3	0.44 × 0.36 × 0.32	0.38 × 0.23 × 0.12
ρ_{calcd} (g/cm^{-3})	1.737	1.845
μ(Mo Kα), mm^{-1}	0.648	1.794
range of transm factors	0.55−0.84	0.52−0.74
data/restraints/params	6150/0/518	6146/63/575
R1 ($I > 2\sigma I$)	0.0360	0.0373
wR2 (all data)	0.0420	0.0450

Scheme 1. Ligand Preparation

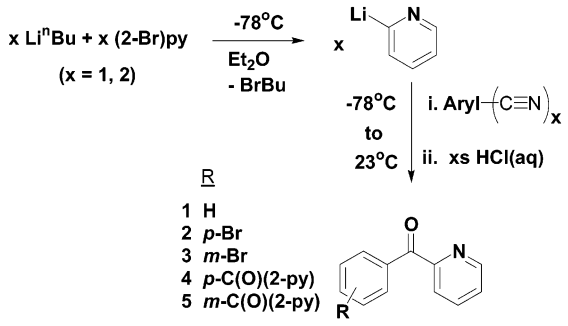

possessed any crystallographically imposed symmetry. One of the PF_6^- counterions was disordered over two nearby positions in the proportions P2A/P2B = 0.69(1)/0.31. The geometries of both disorder components of P2 were restrained to be similar to the ordered anion P1 (SHELX SAME command, 63 restraints). For each data set, all non-hydrogen atoms were refined with anisotropic displacement parameters; hydrogen atoms were placed in geometrically idealized positions and refined as riding atoms with isotropic displacement parameters. Other pertinent crystallographic information for each compound can be found in Table 1.

Results and Discussion

Syntheses of Compounds. The ligands **2**−**5** were prepared by utilizing the reaction between either bromobenzonitrile or dicyanobenzene and 2-lithiopyridine (formed in situ) in either a 1:1 or a 2:1 mol ratio, as appropriate, followed by acid hydrolysis of the lithio-imines as shown in Scheme 1. With the reactions involving bromobenzonitriles, the desired products were obtained in good yield (ca. 70%); however, small amounts of BrPhC(O)PhC(O)py (presumably a result of lithium-aryl exchange prior to reaction with nitrile functionality) were also isolated. While an alternate, potentially higher yielding (45% overall) multistep route to **5** has been described in the literature,[15] the one-pot, two-step procedure analogous to that described for **2** was used for the preparation of **4** and **5**. In these cases, **4** and **5** were each typically isolated in 15−33% yield.

The ruthenium complexes **6**−**10** and [Ru(bpy)$_3$][PF$_6$]$_2$ were prepared in about 70% yield by following the two-step method outlined in Scheme 2. We have found that this method of preparation described recently by Ward and Lahiri[16] is more desirable than the direct reaction between the ligand and Ru(bpy)$_2$Cl$_2$, followed by ion exchange because the former method does not require tedious chromatographic separation of products. The title compounds are all soluble in acetonitrile and to a lesser extent in acetone but only slightly soluble in CH_2Cl_2. Attempts to prepare the monometallic derivatives [(L)Ru(bpy)$_2$][PF$_6$]$_2$ where L = **4** or **5** by the described method have been unsuccessful as only the bimetallic derivatives **9** and **10** were isolated.

Scheme 2. Preparation of Ruthenium Derivatives

$$Ru(bpy)_2Cl_2\cdot 2H_2O + 2\ AgPF_6 \xrightarrow[-\ 2\ AgCl\ -\ 2\ H_2O]{EtOH,\ \Delta\ 2h} [Ru(bpy)_2(EtOH)_2][PF_6]_2 \quad (1)$$

$$[Ru(bpy)_2(EtOH)_2][PF_6]_2 + L \xrightarrow[-2\ EtOH]{\Delta\ 16h} [(L)Ru(bpy)_2][PF_6]_2 \quad (2)$$

L = 1-3, or 2,2'-bpy (one equivalent)
L = 4 or 5 (half-equivalent)

Solid State Structures. ORTEP diagrams of the cations of **6** and **7** are shown in Figure 2. A summary of important bond distances and angles for each compound are given in Table 4. The complexes share some common structural features. The metal center in each compound exhibits a distorted octahedral coordination environment as a result of the small bite angles of the bipyridyl (∼79°) and benzoylpyridine ligands (∼78°). Furthermore, each cation contains one short Ru−N bond of ca. 2.03 Å that is located trans to the oxygen of the benzoylpyridine ligand. The remaining four Ru−N bond distances range between 2.05 and 2.07 Å and are typical of those found in other ruthenium compounds with pyridyl-based ligands. The phenyl and bromophenyl rings are rotated 41.4(4)° and 35.2(8)°, respectively, out of the plane of conjugation with the respective C(O)(2-py)Ru moiety. Moreover, the C(O)(2-py)Ru heterocycles deviate from planarity by a torsion of the C−N and C−O bonds about the connecting C−C bond [4.8(4)° in the case of **6** and 12.1(8)° for **7**]. Intraligand bond distances for the bipyridyl groups are comparable to those observed for [Ru(bpy)$_3$](PF$_6$)$_2$.[17] To the best of our knowledge, *trans*-[PhC(O)(2-py)Ru(PMe$_3$)$_2$(CO)(COMe)]BPh$_4$ (**A**)[11] represents the only other example of a structurally characterized ruthenium−arylpyridylmethanone complex. In **A**, the ruthenium−oxygen and ruthenium−nitrogen bond distances of 2.226(4) and 2.198(4) Å are much longer than those found in **6** [2.0578(19), 2.047(2) Å] and in **7** [2.081(4), 2.064(5) Å]. These unusually long distances in **A** were attributed to the strong trans influence of the CO and COMe ligands.[11] Interestingly, the C−O bond lengths of the arylpyridylmethanone ligands at 1.250(3) Å in **6** and 1.258(7) Å in **7** are comparable to 1.243(6) Å for **A**.

(16) Chakraborty, S.; Laye, R. H.; Paul, R. G.; Gonnade, R. G.; Puranik, V. G.; Ward, M. D.; Lahiri, G. K. *J. Chem. Soc., Dalton Trans.* **2002**, 2348.
(17) Biner, M.; Burgi, H.-B.; Ludi, A.; Rohr, C. *J. Am. Chem. Soc.* **1992**, *114*, 5197.

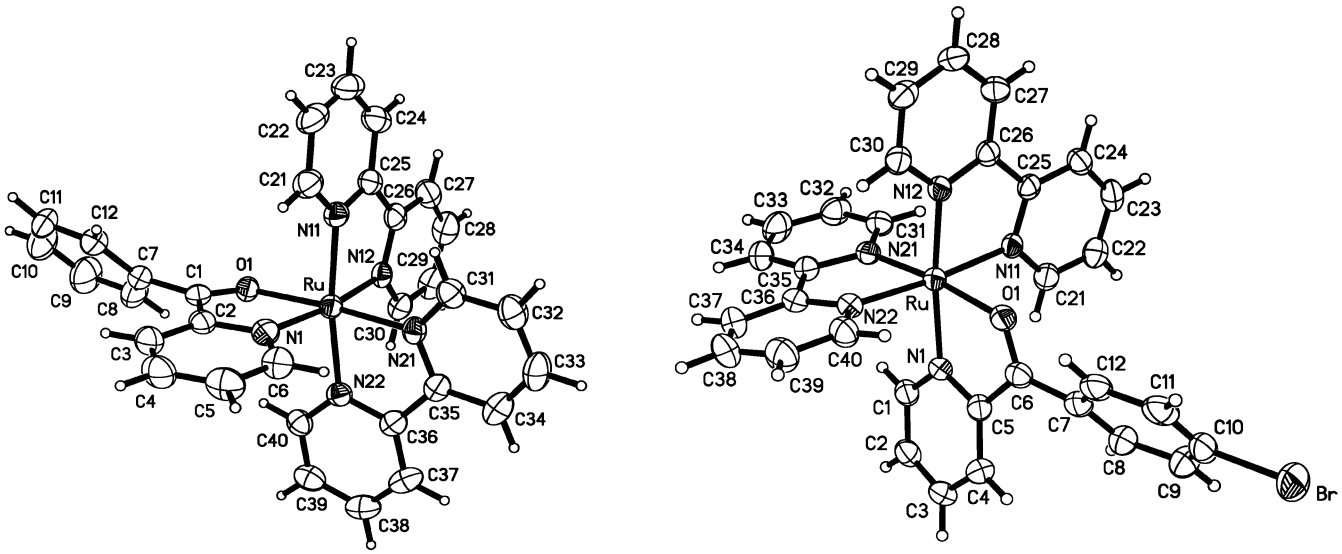

Figure 2. ORTEP plots of cations of $[PhC(O)(2\text{-py})Ru(bpy)_2][PF_6]_2$ **(6)** and $[p\text{-}BrC_6H_4C(O)(2\text{-py})Ru(bpy)_2][PF_6]_2$ **(7).** Ellipsoids drawn at the 50% probability level.

Table 2. Yield and Selected Characterization Data for Ruthenium Aryl(2-pyridyl)methanones

compound	yield (%)	mp[a] (°C)	C,H, N anal. calcd (obsd)	EI(+) MS *m*/*z* calcd (obsd)
$[PhC(O)(2\text{-py})Ru(bpy)_2][PF_6]_2$, (**6**)	71.6	316−318	C, 43.35 (43.88); H 2.84(2.73); N 7.90(7.98)	298.5550 (298.5540) [M^{2+}]
$[p\text{-}BrC_6H_4C(O)(2\text{-py})Ru(bpy)_2][PF_6]_2$ (**7**)	74.4	320−322	C, 39.81 (39.66); H 2.51(2.37); N 7.25(7.13)	
[*m*-Br $C_6H_4C(O)(2\text{-py})Ru(bpy)_2][PF_6]_2$ (**8**)	64.3	301−304	C, 39.81 (39.76); H 2.51(2.43); N 7.25(7.26)	821.9848 (821.9859) [$(M^{2+})(PF_6^-)$]$^+$
$\{p\text{-}[C(O)(2\text{-py})_2Ru(bpy)_2]_2(C_6H_4)\}[PF_6]_4$ (**9**)	62.6	315−318	C, 41.10 (41.41); H 2.62(2.51); N 8.26(8.33)	351.0664 (351.0651) [M^{2+}]
$\{m\text{-}[C(O)(2\text{-py})_2Ru(bpy)_2]_2(C_6H_4)\}[PF_6]_4$ (**10**)	68.5	298−300	C, 41.10 (41.42); H 2.62(2.47); N 8.26(8.21)	

[a] Decomposition.

Table 3. Absorption and Electrochemical Data for Ruthenium Aryl(2-pyridyl)methanones and for $[Ru(bpy)_3][PF_6]_2$ in CH_3CN

		$E_{1/2}$ in V ($E_a - E_c$ in mV)[b]			
compound	λ_{max} (log ϵ)[a]	oxidation[d]		reduction	
$[PhC(O)(2\text{-py})Ru(bpy)_2][PF_6]_2$	436 (3.13), 564 (3.17)	1.38 (86)	−0.58 (80)	−1.36 (73)	−1.53 (84)
$[p\text{-}BrC_6H_4C(O)(2\text{-py})Ru(bpy)_2][PF_6]_2$	434 (3.18), 564 (3.25)	1.37 (102)	−0.53 (84)	−1.36 (79)	−1.51 (78)
[*m*-Br $C_6H_4C(O)(2\text{-py})Ru(bpy)_2][PF_6]_2$	432 (3.12), 564 (3.17)	1.37 (108)	−0.50 (79)	−1.32 (77)	−1.52 (74)
$\{p\text{-}[C(O)(2\text{-py})_2Ru(bpy)_2]_2(C_6H_4)\}[PF_6]_4$	436 (3.33), 564 (3.41)	1.38 (162)	−0.32 (75) −0.53 (84)	−1.48[c]	
$\{m\text{-}[C(O)(2\text{-py})_2Ru(bpy)_2]_2(C_6H_4)\}[PF_6]_4$	436 (3.46), 556 (3.52)	1.37 (135)	−0.48 (74) −0.60 (73)	−1.41[c]	
$[Ru(bpy)_3][PF_6]_2$	451 (4.26)	1.31 (82)		−1.31 (76)	−1.52 (70)

[a] Metal-based transitions. The ligand-centered transitions centered at 236 and 286 nm are also observed for **6**−**10**. [b] $E_{1/2} = (E_a - E_c)/2$. [c] Chemically irreversible, anode potential is reported. [d] In **6**−**10**, small chemically irreversible cathodic peaks centered near +0.25 V were observed.

Supramolecular Structure. The extended structure of **6** is that of sinusoidal chains of cations that lie parallel to the *ac* plane as is shown in Figure 3a. The chains consist of cations of alternating chirality (Λ, Δ, Λ, etc.). Two adjacent cations are organized in pairs by face-to-face $\pi-\pi$ stacking interactions between bipyridyl groups (Figure 3b, blue dashed lines). A pair of cations is connected to two other pairs to form the strand by edge-to-face CH$-\pi$ (Figure 3b, green dashed lines) interactions between bipyridyl groups and by close H···F contacts between atoms of the hexafluorophosphate anions and the hydrogens on the benzoylpyridine ligands. In the $\pi-\pi$ interactions, the pyridyl groups deviate from coplanarity by 4.32° giving an interplane separation minimum of 3.34 Å and maximum of 3.50 Å. The mean slip angle β of 32.9° (concentricity provides a slip angle of 0°) gives a centroid-to-centroid distance of 4.08 Å which is outside the typical values of 20° and 3.8 Å.[18] However, the

Table 4. Selected Bond Distances and Angles for **6**·0.5CH_3CN and **7**

compound	**6**·0.5CH_3CN	**7**
	Bond Distances	
Ru−O(1)	2.0578(19)	2.081(4)
Ru−N(1)	2.047(2)	2.064(5)
Ru−N(11)	2.062(2)	2.069(5)
Ru−N(12)	2.056(2)	2.054(5)
Ru−N(21)	2.030(2)	2.030(5)
Ru−N(22)	2.048(2)	2.044(5)
C(1)−O(1)	1.250(3)	1.258(7)
	Bond Angles	
N(1)−Ru−O(1)	77.48(9)	77.94(17)
N(11)−Ru−N(12)	78.67(9)	78.79(19)
N(21)−Ru−N(22)	79.04(10)	79.0(2)
O(1)−Ru−N(21)	175.55(8)	175.55(8)
N(1)−Ru−N(12)	171.61(9)	171.61(9)
N(11)−Ru−N(22)	171.38(9)	171.38(9)
O(1)−Ru−N(11)	87.90(8)	86.14(17)
N(12)−Ru−N(21)	88.93(9)	90.11(18)
N(22)−Ru−O(1)	98.19(9)	97.67(17)

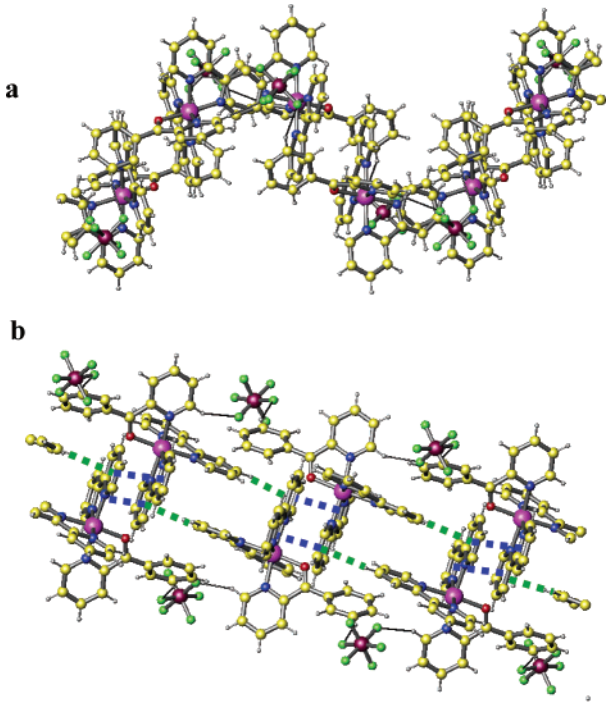

Figure 3. (a) View of sinusoidal chain of cations in **6** that runs along *c* axis. (b) View into *bc* plane emphasizing interactions within chains.

bipyridyl groups are also offset by 25° such that the minimum distance and angle between planes of interacting moieties occurs from the centroid of the entire bpy ligand of one cation and the centroid of only one-half of the second bpy ligand (3.69 Å and 17.0°). In the edge-to-face CH$-\pi$ interaction, the pyridyl group that is positioned trans to the oxygen atom in the coordination sphere of ruthenium is the hydrogen donor while the pyridyl group that is trans to the pyridine group of benzoylpyridine ligand in an adjacent cation of opposite chirality is the hydrogen acceptor. The corresponding CH$-$centroid distance of 2.92 Å and the C$-$H$-$centroid angle of 134.1° are well within the typically accepted ranges for such an interaction.[19] Finally, the chain is further supported by short H$\cdots$F contacts in which a hexafluorophosphate acts as a bridge between the pyridyl moiety of the benzoylpyridine ligand of one cation pair and the phenyl fragment of the benzoylpyridine ligand on a second adjacent cation pair (Figure 3b black lines). These H$\cdots$F contacts of 2.45 and 2.47 Å for H(4)$\cdots$F(4) and H(8)$\cdots$F(8) (from the calculated positions of the hydrogens) are shorter than the sum of the van der Waals radii of the respective atoms (2.54 Å)[20] with associated C$-$H$\cdots$F angles of 161.2° [C(4)$-$H(4)$-$F(4)] and 162.3° [C(8)$-$H(8)$-$F(3)] that are in good agreement with the typical geometric values ($<$2.6 Å and $>$130°) proposed to be indicative of weak hydrogen bonding interactions.[21]

The supramolecular structure of **7** demonstrates that a simple modification of the benzoylpyridine ligand (substitution of hydrogen with bromine at the para position of the phenyl group) noticeably alters the organization of [Ru(bpy)$_2$(ligand)] dications from a simple sinusoidal chain structure to that of a two-dimensional corrugated sheet (Figure 4). As seen in **6**, sinusoidal chains are formed in **7** (Figure 4a) as a result of both CH$-\pi$ and $\pi-\pi$ stacking interactions between bipyridyl groups (Figure 4b, red and blue dashed lines, respectively). In the CH$-\pi$ interaction, the pyridyl group which acts as the hydrogen acceptor is disposed trans to the nitrogen donor atom of the C(O)(py) moiety. The pyridine ring that is bound to the pyridyl group positioned trans to oxygen acts as the hydrogen donor. In this interaction, the H(38)$-$centroid distance of 2.95 Å and the associated C(38)$-$H(38)$-$centroid angle of 138.25° represent typical values.[19] The bipyridyl ligands that act as hydrogen acceptors for the CH$-\pi$ interaction are also involved in a $\pi-\pi$ stacking interaction with an adjacent cation of opposite chirality (blue lines, Figure 4b). The geometry of the stacking arrangement is such that the two involved bipyridyl groups deviate 3.89° from coplanarity where the minimum and maximum perpendicular separations are 3.37 and 3.45 Å, respectively. The centroid-to-centroid distance between the interacting pyridyl groups is 3.667(4) Å which gives a mean slip angle, β, of 21.6°. The major difference in the structure of **7** when compared to **6** is the $\pi-\pi$ stacking of bromophenyl groups that provides connectivity in a second dimension, thus affording sheets, as exemplified by the black dashed lines in Figure 4b. The coplanar bromophenyl groups that are involved in the $\pi-\pi$ stacking interaction are separated by perpendicular distance of 3.34 Å and a centroid-to-centroid distance of 3.91 Å, which gives a deviation from

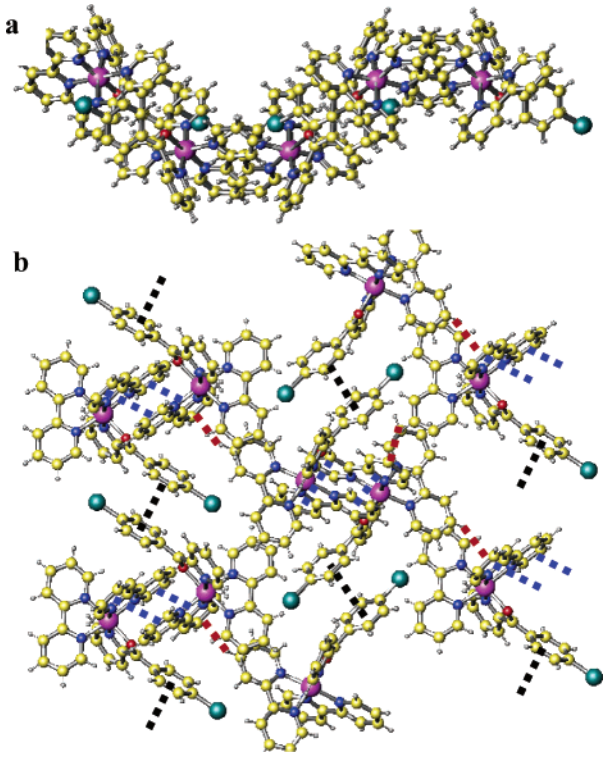

Figure 4. (a) View of extended structure of **7** emphasizing the sinusoidal chain structure. (b) Two-dimensional sheet structure (90° rotation of view a).

(18) Janiak, C. *J. Chem. Soc., Dalton Trans.* **2000**, 3885.
(19) Takahashi, H.; Tsuboyama, S.; Umezawa, Y.; Honda, K.; Nishio, M. *Tetrahedron* **2000**, *56*, 6185.
(20) (a) Bondi, A. *J. Phys. Chem*, **1964**, *68*, 441. (b) Rowland, R. S., Taylor, R. *J. Phys. Chem.* **1996**, *100*, 738.
(21) Grepioni, F.; Cojazzi, G.; Draper, S. M.; Scully, N.; Braga, D. *Organometallics* **1998**, *17*, 296.

concentricity (β) of 31.5°. The observation of this $\pi-\pi$ stacking interaction between aryl moieties in **7**, but not in **6**, is consistent with the expected ability of the electron withdrawing bromine group relative to a hydrogen to induce a greater polarization of the arene.[26] This polarization increases the ability for arenes to become involved in $\pi-\pi$ stacking interactions in accord with Hunter−Sanders rules.[27] Disorder of one of the PF_6^- anions prohibited a complete examination of CH···F interactions; however, two short contacts exist between fluorine atoms of the well-behaved anion and the hydrogen atoms of the pyridyl group disposed trans to the pyridine ring of the bromobenzoylpyridine ligand [F(5)···H(30)C(30) 2.40 Å, 143.9°; F(6)···H(28)C(28) 2.42 Å, 122.7°].

Satisfactory single crystals of **8** for crystallographic studies could not be obtained because of the highly anisotropic morphology (long, exceedingly thin needles). Numerous attempts to obtain suitable crystals of **9** and **10** were also unsuccessful. Crystals showed anisotropic morphology (small thin plates) and extensive twinning, most likely because of the presence of both the homochiral (Λ,Λ and Δ,Δ) and heterochiral (Λ,Δ and Δ,Λ) forms.

Solution Studies

NMR. In order to make an appropriate evaluation of reaction kinetics as monitored by NMR spectrosopic methods and to provide a reference for the identification of more complex ruthenium derivatives, careful assignments of the resonances in the NMR spectra of **6**−**10** were achieved by using a combination of advanced NMR techniques and by taking into consideration the coordination environment about ruthenium (vide infra). The ^{1}H and ^{13}C NMR spectral data obtained for freshly prepared CD_3CN solutions of compounds **6**−**10** are collected in Tables 5 and 6. The assignments for the resonances of each spectrum follow from the labeling scheme exemplified for **6** in Figure 5. Because of the lack of symmetry elements at the metal center, the ^{1}H NMR spectra for compounds **6**−**10** are complicated owing to the presence of multiple overlapping resonances in the aromatic region. In addition to the resonances for aryl hydrogens, the ^{1}H NMR spectra of **6** was expected to consist of five sets of four multiplet resonances for pyridine ring hydrogens: one set (A) for the benzoylpyridine ligand, one set (B) for the pyridine ring situated trans to oxygen of the bound carbonyl group, one set (C) for the ring trans to the nitrogen atom of benzoylpyridine, and one set each for the rings bound to B and C. Homonuclear *J*-resolved experiments clearly showed the existence of the expected five sets of pyridyl resonances (Figure 6), and the spectral data were used to verify the chemical shifts, multiplicities, and coupling constants of each resonance. The resonances that were associated with each of the five pyridyl spin systems were identified from DQCOSY spectral data. The identity of ring A was established from the cross-peaks obtained from gHMBC experiments because of the long-range interactions between H_3(A) and C═O. The cross-peaks obtained from gHMBC experiments also established the connectivity between rings B and E and between C and D as a result of long-range intraligand interactions between H_4, H_5, and H_6 of one ring with C_2' of the second (adjacent) ring. It should be noted that there was no evidence for long-range interligand interactions mediated

Table 5. ^{1}H NMR Spectral Data (500 MHz CD_3CN) for Ruthenium Compounds[a]

		chemical shift δ (ppm)				
		pyridyl group[b,c]				
compound	ring	H_3	H_4	H_5	H_6	aryl
[PhC(O)(2-py)Ru(bpy)$_2$]-[PF$_6$]$_2$ (**6**)	A	8.64	8.153	7.718	7.97	$7.92_{2,6}$ ps d (ortho)
	B	8.533	8.14	7.57	8.21	$7.63_{3,5}$ ps dd (meta)
	C	8.525	8.145	7.53	7.77	7.78_4 ps t (para)
	D	8.49	8.047	7.39	7.721	second order
	E	8.51	8.02	7.37	7.74	
[*p*-BrC$_6$H$_4$C(O)(2-py)-Ru(bpy)$_2$][PF$_6$]$_2$ (**7**)	A	8.61	8.151	7.724	7.97	7.83
	B	8.53	8.14	7.56	8.18	7.81
	C	8.52	8.145	7.52	7.71	AA′BB′
	D	8.49	8.04	7.39	7.74	
	E	8.50	8.02	7.37	7.722	
[*m*-BrC$_6$H$_4$C(O)(2-py)-Ru(bpy)$_2$][PF$_6$]$_2$ (**8**)	A	8.64	8.16	7.736	7.97	8.10
	B	8.530	8.145	7.58	8.19	7.92
	C	8.525	8.151	7.52	7.71	7.90
	D	8.49	8.04	7.40	7.736	7.54
	E	8.51	8.03	7.37	7.726	
{*p*-[C(O)(2-py)$_2$Ru(bpy)$_2$]$_2$-(C$_6$H$_4$)}[PF$_6$]$_4$ (**9**)	A	8.64	8.17	7.76	7.99	8.12
	B	8.54	8.149	7.57	8.17	8.11
	C	8.52	8.153	7.53	7.71	
	D	8.48	8.05	7.40	7.75	
	E	8.49	8.04	7.39	7.72	
{*m*-[C(O)(2-py)$_2$Ru(bpy)$_2$]$_2$-(C$_6$H$_4$)}[PF$_6$]$_4$ (**10**)	A	8.59	8.15	7.748	7.98	8.30_2
	B	8.53	8.141	7.55	8.19	$8.24_{4,6}$
	C	8.511	8.144	7.51	7.69	7.85_3
	D	8.47	8.042	7.38	7.745	
	E	8.506	8.035	7.37	7.70	
[*cis*-Ru(bpy)$_2$(CD$_3$CN)$_2$]-[PF$_6$]$_2$	A	8.60	8.26	7.83	9.30	
	B	8.35	7.93	7.24	7.57	

[a] Refer to Figure 5. [b] Each resonance for pyridine hydrogens appears as a ddd with the following coupling constants: H_3 (J = 8.1, 1.4, 0.8), H_4 (J = 8.1, 7.7, 1.4), H_5 (J = 7.7, 5.5, 1.4), and H_6 (J = 5.5, 1.4, 0.8). [c] The chemical shifts of closely overlapping resonances are reported to three decimal places for clarity but may not represent chemically significant values.

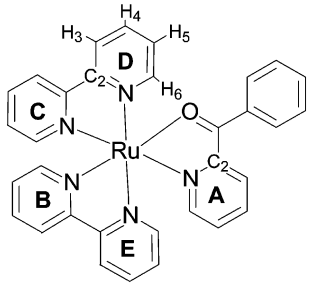

Figure 5. Labeling scheme used for NMR assignments.

(22) (a) Browne, W. R.; O'Connor, C. M.; Villani, C.; Vos, J. G. *Inorg. Chem.* **2001**, *40*, 5461. (b) Hage, R.; Dijkuis, A. H. J.; Haasnoot, J. G.; Prins, R.; Reedjik, J.; Buchanan, B. E.; Vos, J. G. *Inorg. Chem.* **1988**, *27*, 2185.
(23) (a) Durham, B.; Walsh, J. L.; Carter, C. L.; Meyer, T. J. *Inorg. Chem.* **1980**, *19*, 860. (b) Chen, Z. *Gaodeng Xuexiao Huaxue Xuebao* **1987**, *8*, 839.
(24) de Paula, A. S. A. T.; Mann, B. E.; Tfouni, E. *Polyhedron* **1999**, *18*, 2017.
(25) Johnson, E. C.; Sullivan, B. P.; Salmon, D. J.; Adeyemi, S. A.; Meyer, T. J. *Inorg. Chem.* **1978**, *17*, 2211.
(26) (a) Sherman, B. J.; Sen, S.; Galiatsatos, V. *Polymer* **1996**, *37*, 1759. (b) Zou, J.; Yu, Q.; Shang, Z. *J. Chem. Soc., Perkin Trans. 2* **2001**, *8*, 1439. (c) Zhu, W.; Wu, G.-S.; Jiang, Y. *Intl. J. Quantum Chem.* **2002**, *86*, 347.
(27) Hunter, C. A.; Sanders, J. K. M. *J. Am. Chem. Soc.* **1990**, *112*, 5525.

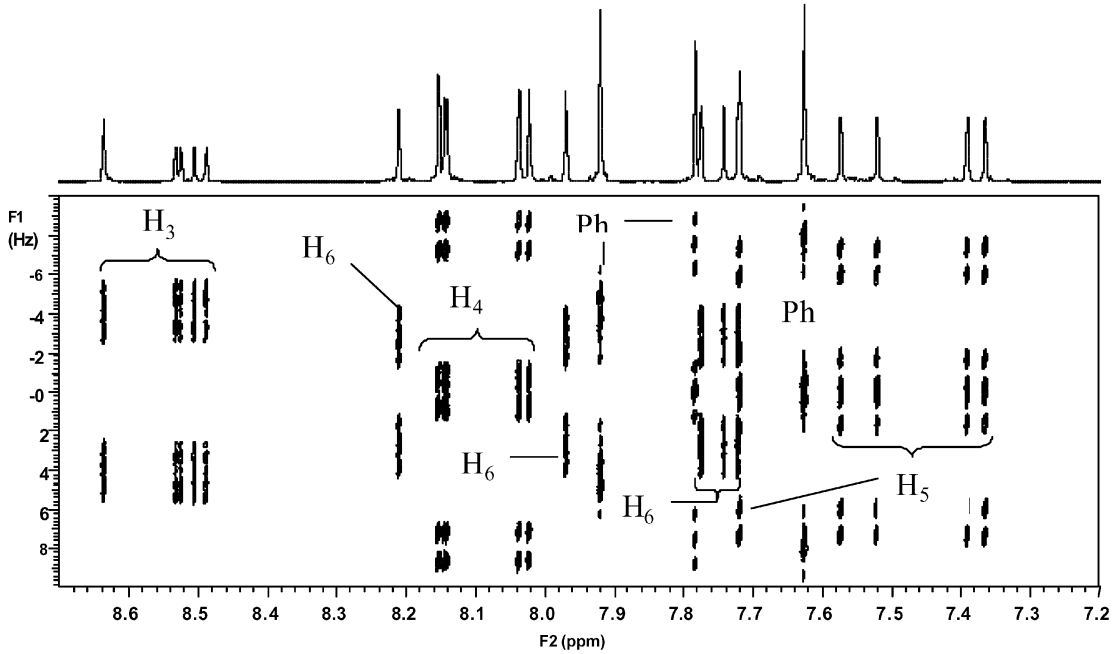

Figure 6. Homonuclear *J*-resolved spectrum of **6** after rotation and with projection.

Table 6. ^{13}C NMR Spectral Data (100.62 MHz CD_3CN) for Ruthenium Complexes

			chemical shift δ (ppm)					
			pyridyl					
compound	C=O	ring	C_2	C_3	C_4	C_5	C_6	aryl[a]
$[PhC(O)(2\text{-py})Ru(bpy)_2][PF_6]_2$ (**6**)	209.4	A	153.85	136.01	138.82	133.54	154.32	135.3_1
		B	157.85	125.23	139.41	128.73	152.80	$131.3_{2,6}$
		C	158.55	125.10	139.76	129.08	153.38	$130.2_{3,5}$
		D	152.09	124.97	139.29	128.14	153.50	136.0_4
		E	152.68	125.56	138.59	128.37	154.09	
$[p\text{-}BrC_6H_4C(O)(2\text{-py})Ru(bpy)_2][PF_6]_2$ (**7**)	208.4	A	153.66	135.87	138.91	133.71	154.40	134.31_1
		B	157.83	125.30	139.41	128.83	152.88	130.82_4
		C	158.60	125.17	139.79	129.14	153.41	133.52_3
		D	158.52	125.05	139.35	128.24	153.49	132.91_2
		E	158.54	125.56	138.61	128.36	154.02	
$[m\text{-}BrC_6H_4C(O)(2\text{-py})Ru(bpy)_2][PF_6]_2$ (**8**)	208.1	A	153.61	136.11	139.01	133.90	154.44	138.50_4
		B	157.83	125.37	139.47	128.89	153.00	137.02_1
		C	158.56	125.09	139.86	129.22	153.50	133.69_2
		E	158.55	125.01	139.42	128.23	153.56	132.06_5
		D	158.54	125.60	138.71	128.43	154.05	130.11_6
								123.65_3
$\{p\text{-}[C(O)(2\text{-py})_2Ru(bpy)_2]_2(C_6H_4)\}[PF_6]_4$ (**9**)	208.7	A	153.38	135.99	138.94	134.03	154.37	139.24_i
		B	157.69	125.30	139.80	128.80	152.80	131.59
		C	158.32	125.59	139.51	129.18	153.41	
		D	158.37	125.00	139.45	128.21	153.50	
		E	158.42	125.09	138.75	128.42	153.87	
$\{m\text{-}[C(O)(2\text{-py})_2Ru(bpy)_2]_2(C_6H_4)\}[PF_6]_4$ (**10**)	208.4	A	153.91	136.13	138.95	134.01	154.54	$136.33_{4,6}$
		B	157.70	125.35	139.91	128.90	152.90	135.90_1
		C	158.37	125.14	139.52	129.20	153.52	132.22_2
		E	158.39	125.01	139.49	128.19	153.59	131.17_5
		D	158.41	125.63	138.77	128.56	154.01	
$[cis\text{-}Ru(bpy)_2(CD_3CN)_2][PF_6]_2$		A	159.03	124.95	139.41	128.56	154.37	
		B	158.24	124.63	139.03	127.79	153.22	

[a] Characters in subscripts refer to position of nuclei on aromatic ring where i refers to ipso.

either through space or through the metal center between nuclei of pyridyl groups. Thus, given that the resonances for ring A were assigned and those for each bpy ligand were identified, consideration of the environment about the metal center provided the basis for completing the assignments, that is, determining the relative position of the two bipyridyl groups in the coordination sphere. That is, the electronic environment of the unique pyridyl group that is disposed trans to oxygen atom in ruthenium's coordination should be more perturbed than those groups disposed trans to pyridyl moieties; hence, the resonances for ring B nuclei should occur at chemical shifts that are more distinct than those of the remaining pyridyl groups. By similar arguments, because each ring D and E are disposed trans to a pyridyl group of the other bipyridine ring whereas ring C is trans to the pyridine ring of benzoylpyridine ligand, resonances for

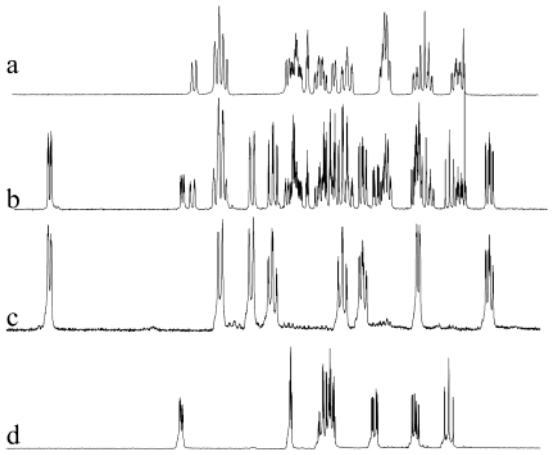

Figure 7. ^{1}H NMR spectra of (a) freshly prepared CD_3CN solution of **8**, (b) same solution after 17 days at 23 °C, (c) freshly prepared CD_3CN solution of $[Ru(bpy)_2(CD_3CN)_2](PF_6)_2$, and (d) of a CD_3CN solution of free ligand **3**.

hydrogens of D an E should have similar chemical shifts. Thus, the spin system (from the COSY experiment) that contained both the second most upfield resonance for each H_3 and H_5 and the most downfield H_6 resonance in Figure 6 was assigned to ring B. Assignment of the second most upfield H_3 resonance (Figure 6) to ring D by these arguments (and by gHMBC) fixes the identity of the remainder of resonances. The assignments for the resonances of compounds **7**−**10** were made by examining the data obtained from a combination of gHMQC and homonuclear *J*-resolved experiments as well as by a comparison with the data for **6**. It should be noted that the spectral data for **9** and **10** were more complicated because of the presence of two magnetically nonequivalent stereoisomers similar those that observed for $\{[Ru(bpy)_2]_2(bpt)\}(PF_6)_3$ where bpt is the uninegative 3,5-bis(2-pyridyl)-1,2,4-triazolyl ligand.[22] This complication is most easily detected by the fact that there is more than one resonance for aryl protons in **9**. Moreover, in both cases, 10 types of pyridyl resonances could be identified from homonuclear *J*-resolved spectra as would be expected for superimposed spectra for homochiral ($\Lambda\Lambda$, $\Delta\Delta$) and heterochiral ($\Delta\Lambda$,$\Lambda\Delta$) derivatives. The data reported for the chemical shifts of pyridyl nuclei in Tables 5 and 6 are the average values of the very closely overlapping resonances. No attempt was made to separate the mixture of isomers and further identify the resonances.

Compounds **6**−**10** are unstable with respect to dissociation of the aryl(pyridyl)lmethanone ligands in CD_3CN solution. After several hours, the ^{1}H NMR spectra begin to show weak intensity resonances for the corresponding free ligand and for $[Ru(bpy)_2(CD_3CN)_2](PF_6)_2$ in addition to those for **6**−**10**. The new resonances grow in intensity at the expense of the original resonances as shown for **8** in Figure 7. The data on the kinetics of dissociation for **8** showed a straight line for the plot of ln[**8**] versus time (see Supporting Information) and indicated that the rate of dissociation is first order in **8** (as might be expected for a 0.019 M CD_3CN solution) with a half-life, $t_{1/2}$, of 15 days ($k = 5.3 \times 10^{-7}$ L mol^{-1} s^{-1}). The rates of dissociation of the other derivatives are qualitatively similar. In light of these results and after considering the nature of the optical and electrochemical properties of $[Ru(bpy)_2(CD_3CN)_2](PF_6)_2$,[23] electrochemical and optical spectroscopic measurements of **6**−**10** in acetonitrile were made as soon as possible after initial dissolution of the solids in CH_3CN.

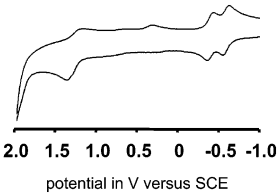

Figure 8. Cyclic voltammogram obtained for **9**.

Optical Data. The spectral data for absorption measurements of **6**−**10** in CH_3CN are collected in Table 3. Aside from two high-energy ligand-based absorption maxima that show a small bathochromic shift when compared to the spectral data of the free arylpyridylmethanone ligands, each of the compounds has two long-wavelength absorption maxima centered near 434 and 564 nm that are assigned to Ru(dπ)−π*(py) and Ru(dπ)−π*[ArC(O)(py)] MLCT transitions, respectively. This assignment is based on the weak intensity of the absorptions and by a comparison with the data reported for $[Ru(bpy)_3](PF_6)_2$ (450 nm)[25] and for [PhC(O)(2-py)Ru$(NH_3)_4$]$(BF_4)_2$ (385, 649 nm) in CH_3CN.[24] Emission measurements of acetonitrile solutions of **6**−**10** from the visible to the near-IR (800−1800 nm) regions indicated that the compounds were nonluminescent under excitation with either 434 or 560 nm light.

Electrochemistry. The electrochemical data for freshly prepared, nitrogen-purged CH_3CN solutions of **6**−**10** and of $[Ru(bpy)_3](PF_6)_2$ are collected in Table 3. The cyclic voltammogram obtained for compound **9** is given in Figure 8 and is representative of those obtained for the remaining ruthenium arylpyridylmethanone derivatives. All of the compounds exhibit metal-based oxidations in the potential range +1.36 to +1.38 V versus SCE as indicated by a comparison of the potential range in the present case with that found for related compounds measured in the same solvent. The oxidations of the metal centers in the homobimetallic derivatives occur at potentials that are indistinguishable and suggest that there is very little to no electronic communication between the metal centers. Oxidation of the metal in each compound appears to be irreversible because the ratio of current intensities of the anode and cathode peaks deviate significantly from the ideal value of 1 and because the measured cathodic/anodic separation potentials were greater than 100 mV. For each compound **6**−**10**, the anode peak of the Ru(II)/(III) couple centered near +1.4 V is easily observed; however, the cathode peak centered near +1.3 V is difficult to observe and, in fact, is absent in the case of compound **6**. These observations combined with the presence of an additional unidentified but reproducible cathodic wave centered near 0.3 V further support the irreversible nature of the oxidation(s). Interestingly, the electrochemical behavior of compound **6** mirrors that described for [PhC(O)(2-py)Ru$(NH_3)_4$]$(BF_4)_2$[24] (**B**) in that the cyclic voltammogram shows an anodic peak attributed to the Ru(II)/(III) couple

which appeared to be irreversible as the cathode peak was either absent or difficult to observe in many solvents including CH_3CN. In the known example **B**, the apparently irreversible nature of the metal-centered oxidation peak was suggested to arise as a result of the high chemical and electrochemical reactivity of the pyridinecarbonyl moiety.[24,28] The nature of the ligand reduction peaks centered near −0.3 to −0.6 V are in accord with values found for related benzoylpyridine compounds.[29]

Conclusions

Five new bis(bipyridyl)ruthenium(II) compounds that incorporate aryl(pyridyl)methanone ligands have been prepared in good yield by the reaction between $[Ru(bpy)_2(EtOH)_2][PF_6]_2$ and the appropriate ligand. Two of the monometallic benzoylpyridine derivatives were characterized by X-ray crystallography which revealed that $\pi-\pi$ and $CH-\pi$ stacking interactions between bipyridyl groups similar to those observed in the β and γ forms of $[Ru(bpy)_3](PF_6)_2$ serve to form chains of cations. Moreover, simple substitution from hydrogen to bromine at the para position of the aryl group is sufficient to allow the aryl group to become involved in $\pi-\pi$ stacking interactions that organize the chains into a sheet structure. Each compound has been fully characterized in acetonitrile solution by a number of NMR spectroscopic methods that allowed full assignment of ^1H and ^{13}C resonances and also demonstrated that the methanone ligands were unstable with respect to dissociation in that solvent. While the optical spectra showed two absorption maxima due to MLCT transitions, the compounds were found to be nonluminescent. Electrochemical data acquired for CH_3CN solutions of the bimetallic derivatives indicate that there is no electronic communication between metal centers mediated either through space or through ligand orbitals.

Acknowledgment. We thank the National Science Foundation (Grant CHE-0110493) for support. The Bruker CCD single crystal diffractometer was purchased using funds provided by the NSF Instrumentation for Materials Research Program through Grant DMR:9975623.

Supporting Information Available: Crystallographic data for $[PhC(O)(2\text{-py})Ru(bpy)_2][PF_6]_2$ **(6)** and $[p\text{-}BrC_6H_4C(O)(2\text{-py})Ru(bpy)_2][PF_6]_2$ **(7)** in CIF format. Plot of kinetic data for ligand dissociation of $[m\text{-}BrC_6H_4C(O)(2\text{-py})Ru(bpy)_2][PF_6]_2$ **(8)** in CD_3CN, ln[**8**] versus time. This material is available free of charge via the Internet at http://pubs.acs.org.

IC026018N

(28) See for instance: (a) Nelson, D. A.; Hayon, E. *J. Phys. Chem.* **1972**, *76*, 3200. (b) Ortica, F.; Elisei, F.; Favarro, G. *J. Chem. Soc., Faraday Trans.* **1995**, *91*, 3405. (c) Albini, A.; Bortolus, P.; Fasani, E.; Monti, S.; Negri, F.; Orlandi, G. *J. Chem Soc., Perkin Trans 2* **1994**, *4*, 691. (d) Elisei, F.; Favaro, G.; Romani, F *Chem. Phys.* **1990**, *144*, 107. (e) Stocker, J. H.; Jenevein, R. M. *J. Org. Chem.* **1969**, *34*, 2807.

(29) Leventis, N.; Elder, I. A.; Gao, X.; Bohannan, E. W.; Sotiriou-Leventis, C.; Rawashdeh, A. M. M.; Overschmidt, T. J.; Gaston, K. R. *J. Phys. Chem. B.* **2001**, *105*, 3663.